PHYSICAL REVIEW A VOLUME 56, NUMBER 4 OCTOBER 1997

Aspects of postcollision interactions near the Ar L shell

James A. R. Samson, Y. Lu, and W. C. Stolte
Behlen Laboratory of Physics, University of Nebraska, Lincoln, Nebraska 68588-0111
(Received 2 May 1997)

In the present work we are interested in near-threshold photoionization experiments involving postcollision effects related to the Auger decay of a vacancy in the Ar L shell. In particular, we have measured the photoelectron energy spectrum resulting from the above postcollision interaction effects and have observed electrons produced by the process of electron capture and reemission. [S1050-2947(97)51110-3]

PACS number(s): 32.80.Hd, 32.80.Dz, 32.80.Fb, 32.50.+d

When an inner-shell $2p$ photoelectron is ejected from the L shell of Ar, the resulting Auger decay leaves the doubly charged ion primarily in its $3s^2 3p^4(^3P, ^1D, ^1S)$ states and to a lesser extent in the $3s3p^5(^3P, ^1P)$ states [1,2]. When photoionization takes place just above the L-shell threshold a slow photoelectron is produced receding away from the singly ionized core. Subsequent decay of the vacancy produces a fast Auger electron. If the lifetime of the inner-shell vacancy is sufficiently short the fast Auger electron can overtake the photoelectron, which is then exposed to a doubly charged ion core. The photoelectron will be retarded losing a certain amount of energy, whereas the Auger electron (now exposed to a singly charged core) gains energy. This exchange of energy results in a distorted line shape and a shift in the peak energy of both electrons and is called a postcollision interaction (PCI) [3–5]. Near-threshold studies have not observed any unaffected Auger lines [6]. This implies that all the interacting photoelectrons will experience a loss in their initial kinetic energy E_k. If this is the case then no threshold photoelectrons ($E_k=0$) can escape and the probability for recapture would be 100% at threshold. Eberhardt *et al.* [7] and Tulkki *et al.* [8] calculated the relative probability for electron recapture as a function of the energy of the incident photons. Normalizing their results at the L_2 threshold they found good agreement with their Ar^+ measurements above the L_2 threshold. We find that their normalized data are also in good agreement with our recent Ar^+ data [9]. This has explained the presence of the anomalous Ar^+ continuum produced in an Auger decay. But the presence of a large Ar^{2+} continuum starting at threshold and continuing to increase at higher energies remains to be explained. Similar large increases in the double-ionization signal have been observed at the inner-shell thresholds of O, Ar, Kr, and Xe [7,10–12]. Because of electron recapture we would expect the Ar^{2+} signal to be zero at threshold. In Ref. [9] we used our experimental curve as a universal recapture probability curve to predict the probability for electron capture into autoionizing levels of the Ar^+ satellite core states produced during the Auger decay. These states would then decay by reemitting the captured electrons with various discrete energies. This electron capture and reemission process can then explain the continuity of the Ar^{2+} signal across the $L_{2,3}$ threshold. This report describes the observation and analysis of electron capture and reemission.

The photoionization measurements were made at the Advance Light Source in Berkeley, CA, on the undulator beamline 9.0.1 and on the bending magnet beamline 6.3.2. The photon-energy range used lay between 240 and 255 eV and the photon-energy resolution ranged from 40 to 120 meV. Fluorescence measurements were made in the visible spectrum with a broad bandpass filter covering the range 360–425 nm. The fluorescent chamber was simply an integrating sphere [13], 10 cm in diameter and coated internally with an extremely high reflectance material. The integrated signal was recorded with an RCA 8850 photomultiplier. The photoelectron spectra were measured using a 180° spherical electron energy analyzer (mean radius of 5 cm) between 0 and 6 eV with a resolution of 40 to 100 meV.

As mentioned earlier the normal Auger decay produces a doubly charged ion primarily in a $3s^2 3p^4$ (^3P, ^1D, or ^1S) state [1,2]. Consider a postcollision interaction between the Auger electron and the outgoing photoelectron that produces electron capture. Then states such as $3s^2 3p^4(^3P)nl$ or $3s^2 3p^4(^1D)nl$, etc., will be formed. If the photoelectron is captured in any orbital below the double-ionization continuum no autoionization can occur and the state must relax by fluorescence leaving the ion in a singly charged state. The visible fluorescent radiation emitted as a function of the incident photon energy is compared with the Ar^+-ion signal in Fig. 1. There is a small continuous background in each spectrum that is produced by direct ionization and/or excitation of the Ar valence electrons. The zero signal level is shown in both cases by the solid base line. The similarity between the two spectra above the $^2P_{1/2}$ limit leaves little doubt that the Ar^+ continuum is created by electron capture into Ar^+ satellite states that subsequently fluoresce in the visible and vacuum uv spectral regions. The $4s$ level can fluoresce only in the vacuum ultraviolet region [14]. Thus the small visible signal observed must be caused by shake-up of $4s \rightarrow 5s$, as predicted by theory [15].

Photoelectrons captured into orbitals above the double-ionization continuum can autoionize into several available continua through a valence multiplet Auger decay [16–18]. Figure 2 illustrates these possibilities for the $(^1D_2)nd'$ and $(^1S_0)md''$ levels, where $n \geqslant 6$ and $m \geqslant 5$. Figure 3 shows the Ar^{2+}-ion signal in the vicinity of the argon L shell [9]. The shaded areas represent our predicted probability for ion production through the process of electron capture and reemission, where a probability of 100% occurs at threshold. Details are discussed in Ref. [9]. The nonshaded areas below the dashed lines represent the amount of true photoelectrons that are ejected, although with distorted line shapes and peak

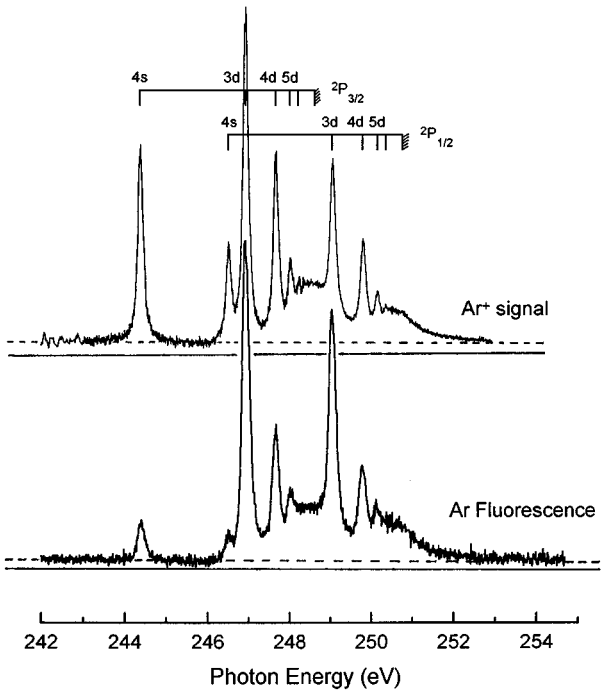

FIG. 1. Comparison of Ar^+-ion yield and fluorescence as a function of photon energy. The solid lines indicate zero signal. The dashed lines indicate the contribution from direct ionization and/or excitation of the Ar valence electrons.

energy shifts. At the $L_{2,3}$ thresholds all zero-energy photoelectrons must be captured; therefore, no Ar^{2+} ion signal should be seen. Note, as in the Ar^+ and fluorescent spectra (Fig. 1), there is a small continuous Ar^{2+} signal caused by direct double ionization of the Ar valence shell. The cross section of this continuum steadily decreases as a function of photon energy from its maximum at about 100 eV [19,20]. In the vicinity of the Ar $2p$ resonances our measurements gave

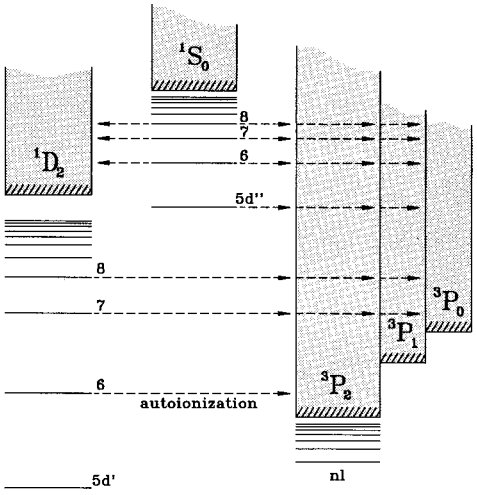

FIG. 2. Energy-level diagram of the $Ar^{2+}(^3P, ^1D, ^1S)$ continua. The discrete Rydberg states leading up to double ionization represent the Ar^+ satellite states.

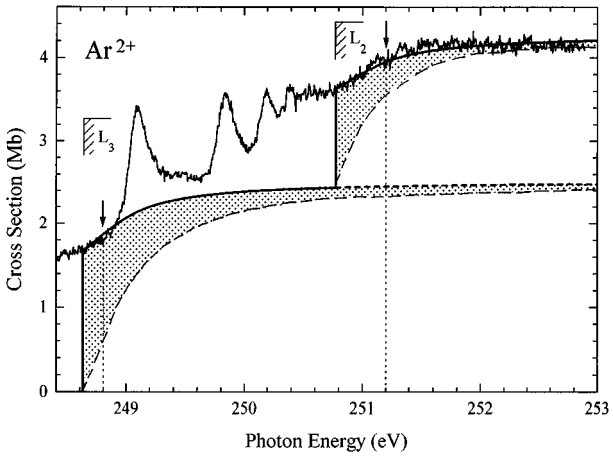

FIG. 3. The Ar^{2+}-ion signal in the vicinity of the L shell [9]. The shaded areas represent the predicted fraction of the total Ar^{2+} continuum that is produced through electron capture and reemission. The vertical arrows and vertical dashed line indicate the regions studied in the present work.

a cross section of 0.02 Mb, which have been subtracted from the data shown in the figure. The experimental data in Fig. 3 show continuity of the Ar^{2+} signal across the L edge. This can be explained on the basis of electron capture and reemission. Another possibility would require double Auger or shake-off processes coupled with electron capture into a low-lying orbit that could only fluoresce, but then no autoionizing electron energy peaks would be observed. We will see that this is not the case.

We have looked for electrons produced by autoionization by measuring the photoelectron spectrum at 248.8 and 251.2 eV. The results obtained at 248.8 eV are shown in Fig. 4. The entire autoionization spectrum of the $(^1D)nd'$ satellite state from $n=6$ to infinity is observed. The collection effi-

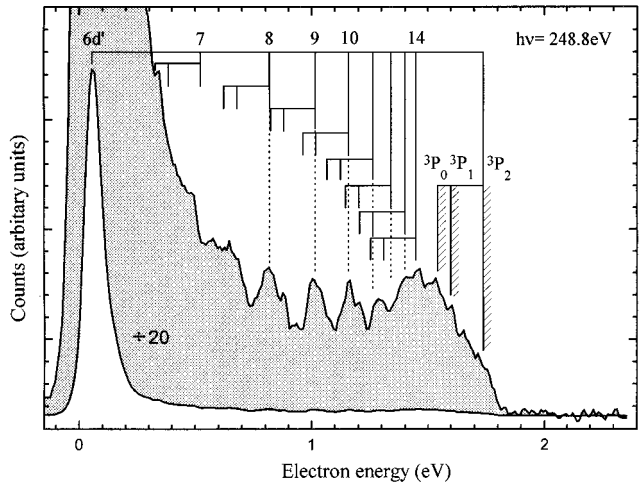

FIG. 4. The photoelectron spectrum of Ar at 248.8 eV. The amplitude of the $6d'$ line has been divided by 20. Note that the resolution of the autoionized lines depend only on the resolution of the energy analyzer (~100 meV) and not on the photon-energy resolution (~120 meV). Note: the shading has no relationship to Fig. 3.

ciency for low-energy electrons (e.g., the $6d'$, 50-meV electron) was about 100 times greater than that for the other electrons. Thus the absolute intensity of the $6d'$ peak is comparable to that of the other peaks. The termination of the nd' photoelectron spectrum at 1.74 eV through autoionization into the $^3P_2$ continuum (the energy difference between the ^1D and $^3P_2$ thresholds) is independent proof that this series is the major contributor to the autoionization spectrum. The widths of the observed lines depend on the intrinsic widths of the autoionizing states [18,21] and on the resolution of the electron-energy analyzer, which was set for 100 meV for this spectrum. This resolution is insufficient to separate the contributions from autoionization into the $^3P_0$ and $^3P_1$ continua, which is 57 meV. From Fig. 4 we can estimate only that the intrinsic widths of the nd' states may be less than 100 meV, based on the fact that the sharpest line in the spectrum ($6d'$) has a width equal to the instrumental width. Changing the resolution of our analyzer to 50 meV also changed the observed width of the $6d'$ line to 50 meV. Thus, we can conclude that the intrinsic width of the $6d'$ line is less than 50 meV. We note that from Fig. 3 we would have expected a single small photoelectron peak at 170 meV. However, the PCI effect can retard the photoelectron peaks by as much as 100–200 meV to lower energies [22,23]. The slight asymmetry on the high-energy side of the $6d'$ peak is likely to be caused by this photoelectron peak.

Repeating the photoelectron measurements at 251.2 eV we would expect to see (in the absence of any PCI effects) only two narrow photoelectron peaks located at 0.42 eV ($2p_{1/2}$) and at 2.37 eV ($2p_{3/2}$). Figure 5 shows our results. The expected positions of these peaks are indicated by the vertical dashed lines. The $2p_{3/2}$ peak position is retarded by 0.15 eV from its expected position and has a low-energy tail giving the peak a half-width of 0.43 eV instead of the expected 0.16 eV caused by the photon resolution, natural widths of the L_2,L_3 levels, and energy analyzer resolution. The $2p_{1/2}$ peak appears to be retarded by about 0.20 eV and can be seen partially emerging from the overlapping $6d'$ autoionizing peak (dotted curve). In addition to the $6d'$ peak we see again the $(^1D)nd'$ satellite states. However, the autoionized peaks are much weaker than the photoelectron peaks, as would be expected from our predicted distribution at 251.2 eV shown in Fig. 3.

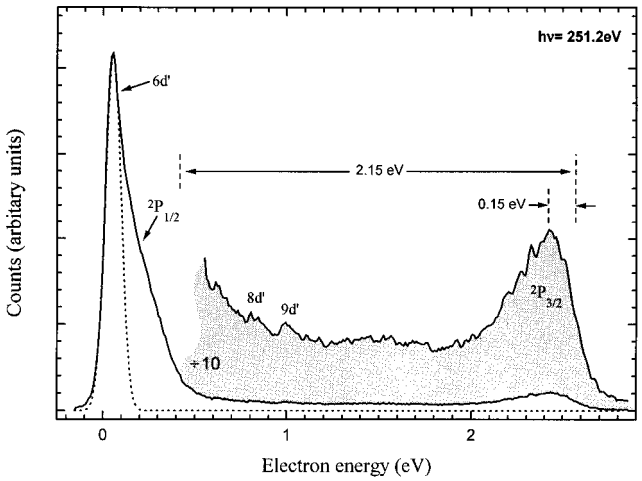

FIG. 5. The photoelectron spectrum of Ar at 251.2 eV. The $2p_{3/2}$ photoelectron is shown broadened and its peak displaced 150 meV to lower energies by PCI effects. Normally the $2p_{1/2}$ and $2p_{3/2}$ photoelectrons must be separated by 2.15 eV, as shown in the figure; however, the $2p_{1/2}$ electron is just starting to appear. Note: the shading has no relationship to Fig. 3.

This work was supported by the National Science Foundation under Grant No. PHY-9317934.

[1] W. Melhorn, Z. Phys. **160**, 247 (1968).
[2] L. O. Werme, T. Bergmark, and K. Siegbahn, Phys. Scr. **8**, 149 (1973).
[3] R. B. Barker and H. W. Berry, Phys. Rev. **151**, 14 (1966).
[4] P. J. Hicks, S. Cvejanović, J. Comer, F. H. Read, and J. M. Sharp, Vacuum **24**, 573 (1974).
[5] H. G. Heideman, G. Nienhuis, and T. Van Ittersum, J. Phys. B **7**, 493 (1974).
[6] J. A. De Gouw, J. van Eck, J. van der Weg, and H. G. M. Heideman, J. Phys. B **25**, 2007 (1992).
[7] W. Eberhardt, S. Bernstorff, H. W. Jochims, S. B. Whitfield, and B. Crasemann, Phys. Rev. A **38**, 3808 (1988).
[8] J. Tulkki, T. Åberg, S. B. Whitfield, and B. Crasemann, Phys. Rev. A **41**, 181 (1990).
[9] J. A. R. Samson, W. C. Stolte, Z. X. He, J. N. Cutler, and D. Hansen, Phys. Rev. A **54**, 2099 (1996).
[10] T. Hayaishi *et al.*, J. Phys. B **17**, 3511 (1984).
[11] P. Lablanquie and P. Morin, J. Phys. B **24**, 4349 (1991).
[12] W. C. Stolte *et al.*, J. Phys. B (to be published).
[13] J. A. R. Samson, E. M. Lee, and Y. Chung, Phys. Scr. **41**, 850 (1990).
[14] J. A. R. Samson, Y. Chung, and E. M. Lee, Phys. Lett. A **127**, 171 (1988).
[15] M. Meyer, E. V. Raven, B. Sonntag, and J. E. Hansen, Phys. Rev. A **43**, 177 (1991).
[16] G. B. Armen and F. P. Larkins, J. Phys. B **25**, 931 (1992).
[17] U. Becker, R. Wehlitz, O. Hemmers, B. Langer, and A. Menzel, Phys. Rev. Lett. **63**, 1054 (1989).
[18] M. Pahler, C. D. Caldwell, S. J. Schaphorst, and M. O. Krause, J. Phys. B **26**, 1617 (1993).
[19] N. Saito and I. H. Suzuki, Int. J. Mass Spectrom. Ion Processes **115**, 157 (1992).
[20] D. M. P. Holland, K. Codling, J. B. West, and G. V. Marr, J. Phys. B **12**, 2465 (1979).
[21] J-P. Connerade and A. M. Lane, Rep. Prog. Phys. **51**, 1439 (1988).
[22] L. Avaldi, R. I. Hall, G. Dawbers, R. M. Rutter, and G. C. King, J. Phys. B **24**, 427 (1991).
[23] V. Schmidt, S. Krummacher, F. Wuilleumier, and P. Dhez, Phys. Rev. A **24**, 1803 (1981).